

# Low-flow-resistance Methacrylate-based Polymer Monolithic Column Prepared by Low-conversion Ultraviolet Photopolymerization at Low Temperature

Tomohiko HIRANO,\* Ayumi KOBAYASHI,\* Takuya NAKAZA,\* Shinya KITAGAWA,\*† Hajime OHTANI,\* Kazuaki NAGAYAMA,\*\* and Takeo MATSUMOTO\*\*

\*Department of Materials Science and Engineering, Graduate School of Engineering, Nagoya Institute of Technology, Gokiso, Showa, Nagoya 466-8555, Japan

\*\*Department of Engineering Physics, Electronics and Mechanics, Graduate School of Engineering, Nagoya Institute of Technology, Gokiso, Showa, Nagoya 466-8555, Japan

A low-conversion poly(butyl methacrylate-*co*-ethylene dimethacrylate)-based polymer monolithic column was prepared by ultraviolet (UV) irradiation for a short time at a low temperature ( $-15^{\circ}\text{C}$ ). By UV irradiation for 2 min, the monolithic column exhibited a high permeability of  $5.6 \times 10^{-13} \text{ m}^2$  and a high column efficiency of over 100000 plates  $\text{m}^{-1}$ . At this polymerization time, the conversions of butyl methacrylate and ethylene dimethacrylate were only 10 and 21%, respectively, as determined by pyrolysis gas chromatography. The low conversion led to high porosity, which in turn resulted in high permeability. The reduction in conversion also contributed to improve the compositional homogeneity of the prepared polymer monolith, which would promote high column efficiency. Using the prepared low-conversion column in conjunction with a vacuum-driven low-pressure HPLC without a conventional high-pressure pump, the separation of alkylbenzenes was successfully achieved using a low pressure of only  $-0.045 \text{ MPa}$  to generate the mobile phase stream.

(Received November 5, 2012; Accepted November 26, 2012; Published February 10, 2013)

## Introduction

In recent years, porous monolithic columns have attracted much attention for use in HPLC.<sup>1-5</sup> Materials suitable for the fabrication of the monolithic bed are divided into two main categories: silica<sup>6-8</sup> and polymer<sup>9-16</sup> monolith. Silica monolithic columns have well-controlled pore structure, good mechanical strength, and high column efficiency,<sup>7,8</sup> while polymer monolithic columns have unique features such as applicability over a wide pH range and simplicity of preparation.<sup>12-16</sup>

One of the most attractive properties of monolithic columns is their low flow resistance resulting from the high permeability of monolithic beds. This high permeability decreases back pressure during separations and enables unique applications that are not possible with conventional packed columns. The low flow resistance allows the column length to be extended significantly.<sup>17,18</sup> Miyamoto *et al.* demonstrated the separation of benzene and its deuterium substitutions using an octadecylsilyl (ODS)-modified silica monolithic column of 12.4 m in length.<sup>17</sup> Another unique application of monolithic columns was ultrahigh-speed separations using a mobile phase stream with a linear flow rate ranging from tens to one hundred  $\text{mm s}^{-1}$ .<sup>19-22</sup>

Low-flow-resistance HPLC columns could be used to construct HPLC systems without the need for conventional LC high-pressure pumps to supply the mobile phase. An open

tubular capillary column is the most permeable (lowest flow resistance) column used in HPLC. Kiplagat *et al.*, using an open tubular capillary column, demonstrated the separation of inorganic anions using a lightweight portable LC system in which the mobile phase was supplied to the column by siphoning with a difference in height of 2 m.<sup>23</sup> Monolithic columns can be used in a similar HPLC system without the need for a high-pressure pump, utilizing gas and/or vacuum pressure-driven pumps instead, when the flow resistance of the monolithic column is sufficiently low and the column efficiency is adequately high. Particularly, a vacuum pressure-driven capillary HPLC with a direct injection method could be used to construct the simplest chromatograph.

Recently, polymer monolithic columns with high separation efficiency and high permeability were developed using new polymerization methods such as low-conversion polymerization<sup>16,24-26</sup> and low-temperature ultraviolet (UV) photopolymerization.<sup>21,22,27</sup> In the former process, the preparation of polymer monoliths using relatively short time thermal-polymerization resulted in increased porosity and specific surface area of the monolith, and column efficiency for small molecules was enhanced along with decreased flow resistance.<sup>16,24-26</sup> In the latter process, photopolymerization of monoliths was carried out at low temperatures ranging from  $-15$  to  $15^{\circ}\text{C}$ .<sup>21,22,27</sup> While the detailed effects of a low polymerization temperature have not been elucidated, it has been reported that photopolymerization under lower temperatures resulted in both higher separation efficiency and higher permeability in monolithic columns.<sup>21,27</sup>

† To whom correspondence should be addressed.

E-mail: kitagawa.shinya@nitech.ac.jp

In this study, we combined these two polymerization methods to prepare polymer monolithic columns; the potential for low-conversion and low-temperature UV photopolymerization to further enhance column efficiency and decrease the flow resistance of methacrylate ester-based polymer monolithic columns were investigated. We previously found that an increase in irradiation intensity in the range from 0.3 to 2.0 mW cm<sup>-2</sup> resulted in enhancement of both column efficiency and permeability.<sup>21</sup> Accordingly, a high-pressure Hg lamp (an irradiation intensity of 170 mW cm<sup>-2</sup>) was used as a high-power light source for photopolymerization in the preparation of the monolithic columns at low polymerization temperature. Here, the effects of the conversion on the chromatographic properties of the prepared columns, such as flow resistance and separation efficiency, were evaluated by varying the polymerization time. Using the fabricated low-flow-resistance monolithic column, we then demonstrated the separation of alkyl benzenes in a vacuum-driven low-pressure HPLC without the need for a conventional high-pressure HPLC pump.

## Experimental

### Chemicals

Butyl methacrylate (BMA), ethylene dimethacrylate (EDMA), 1-decanol, cyclohexanol, 2,2-dimethoxyphenyl-2-acetophenone (DMPA), methanol, acetonitrile (ACN), uracil, toluene, *n*-propylbenzene, *n*-butylbenzene, and *n*-pentylbenzene were purchased from Wako Pure Chemicals (Osaka, Japan). Ethylbenzene was obtained from Tokyo Chemical Industry (Tokyo, Japan). A supply of 3-methacryloxypropyltrimethoxysilane (MAPS) was obtained from Shin-Etsu Chemicals (Tokyo). BODIPY FL C<sub>16</sub> was obtained from Molecular Probes, Inc. (Eugene, OR). All chemicals were used as received.

### Column preparation

A UV-transparent fused silica capillary (100 μm i.d., 375 μm o.d., GL Science, Tokyo, Japan) was silanized with MAPS as described in our previous report.<sup>21</sup> The capillary was cut to 15 cm long and filled with reaction solution consisting of BMA (monomer, 24 wt%), EDMA (cross-linker, 16 wt%), 1-decanol (porogen, 34 wt%), cyclohexanol (porogen, 26 wt%), and DMPA (photoinitiator, 1 wt% with respect to the monomers),<sup>19-21</sup> and the solution was photopolymerized using a high-pressure Hg lamp (170 mW cm<sup>-2</sup>, 365 nm, HLR100T-2, SEN LIGHT Corp., Osaka, Japan) for 1.5 - 16 min in an incubator (MIR-153, Sanyo, Osaka, Japan) at -15, 0, and, 15°C. After polymerization, the columns were immediately washed with methanol to remove unreacted reagents, unfixed-polymer fragments, and porogens.

### Chromatographs

A conventional capillary HPLC system consisting of a pump (LC-10ADvp, Shimadzu, Kyoto, Japan), a sample injector (Model 7520, Rheodyne, Cotati, CA), a T connector equipped with a resistance tube for split injection (split ratio, 1:50), and a UV/Vis detector (CE-1575, Jasco, Tokyo, Japan) was used to evaluate the column characteristics (flow resistance, column efficiency, and retention) with an isocratic elution in the reversed phase (RP)-HPLC mode.

A vacuum-driven HPLC system without a conventional HPLC pump was also used in this experiment. The system was comprised of a sample solution reservoir, a mobile phase reservoir, a polymer monolithic column polymerized for 2 min, a UV/Vis detector (identical to that in the pressure-driven HPLC

mentioned above), a regulator, a stopcock, and a vacuum pump (DAP-6D, ULVAC KIKO Inc., Miyazaki, Japan). A schematic illustration of this system is shown in Fig. S1.

All chromatographic experiments were performed at room temperature.

### Calculation of porosity and permeability of monolithic columns

In general, the linear flow velocity is inversely proportional to the column porosity at a constant volumetric flow velocity. Therefore, column porosity  $\varepsilon$  can be estimated by the following equation:

$$\varepsilon = \frac{u_{sf}}{u_0} \quad (1)$$

where  $u_{sf}$  and  $u_0$  are the  $t_0$ -based linear flow velocities for an open tubular capillary without a monolith (superficial velocity) and for the monolithic column (chromatographic linear flow velocity), respectively.

The permeability  $K$  of a prepared monolithic column can be calculated using the following equation:<sup>28</sup>

$$K = \frac{u_{sf}\eta L}{\Delta P} \quad (2)$$

where  $\eta$ ,  $L$ , and  $\Delta P$  are the viscosity of the mobile phase, the column length, and the pressure drop, respectively.

### Observation of the column cross-section

A longitudinal cross-section of the prepared column was observed using confocal laser scanning microscopy (CLSM, an inverted microscope, TE2000E, Nikon, Tokyo, Japan) combined with a confocal laser scanning system (Digital Eclipse C1, Nikon).<sup>29-30</sup> A fluorescent dye was adsorbed onto the monolith according to the following procedure: first, the column was filled with 0.01% BODIPY FL C<sub>16</sub> in ACN to stain the monolith, followed by flushing with 50% ACN aqueous solution (v/v), which is the same composition used for the mobile phase in the isocratic separation mode. The teflon outer coating of the capillary was removed, and the column was cut into pieces about 5 mm in length. A piece of the column was dipped in a 62% KSCN aqueous solution during the CLSM (×40 objective lens) observation to suppress distortion of the images.

### Determination of conversion of the polymer monolith

Pyrolysis gas chromatography (Py-GC) was employed for determination of the monomer conversions and BMA/EDMA ratio of polymer monolith fixed in the column.<sup>31</sup> A vertical microfurnace-type pyrolyzer (PY2020iD, Frontier-Lab, Koriyama, Japan) was directly attached to the injection port of a gas chromatograph (G-6000, Hitachi) equipped with a flame ionization detector. The outer coating of the capillary monolithic column was removed and the bare column was cut to 5 mm long. A piece of the monolithic column was placed in a sample cup and then introduced into the pyrolyzer heated to 450°C under a flow of helium carrier gas (57 mL min<sup>-1</sup>). At the elevated temperature, the poly(BMA-*co*-EDMA) monolith fixed in the column was depolymerized to the constituent monomers, BMA and EDMA. The thermal decomposition products were directly introduced into a GC separation column (1:50 split ratio) through an injection port maintained at 280°C. For the separation of the degradation products, a metal capillary column (Ultra ALLOY+ 1701, Frontier-Lab, 30 m × 0.25 mm i.d. × 0.25 μm coated with 14% cyanopropylphenyl/86% dimethylpolysiloxane, Koriyama, Japan) was used. The

temperature of the column was initially set to 40°C, then elevated to 280°C at a rate of 20°C min<sup>-1</sup>, and maintained at 280°C for 20 min.

The copolymer composition by weight (wt% ratios for BMA and EDMA are denoted as  $r_{\text{BMA}}$  and  $r_{\text{EDMA}}$ , respectively) constituting the monolith was determined based on the peak area ratio of BMA and EDMA in the observed pyrogram.<sup>31</sup> The total weight of the poly(BMA-co-EDMA) monolith contained in a 5-mm length of column was determined as follows: first, a 5-mm section of monolithic column without the outer coating was weighed by micro-balance (UMT2, Mettler Toledo, Greifensee, Switzerland), incinerated using a gas burner to combust the monolith, and weighed again. The weight differential before/after incineration was defined as the total weight of the monolith,  $w$ , fixed in the capillary. We estimated the mass of BMA and EDMA in the reaction solution loaded into the 5 mm capillary as  $W_{\text{BMA}}$  and  $W_{\text{EDMA}}$ , respectively, according to the composition and density of the reaction solution and the volume of the 5 mm capillary.  $W_{\text{BMA}}$  and  $W_{\text{EDMA}}$  would correspond to the weight of monolith in 100% conversion. The conversion %C of each compound was estimated using the following equation:

$$\%C = \frac{w \times r_{\text{BMA or EDMA}}}{W_{\text{BMA or EDMA}}} \times 100 \quad (3)$$

## Results and Discussion

### Characterization of prepared monolithic column

Poly(BMA-co-EDMA) monolithic columns were polymerized by UV irradiation for various time periods (1.5, 2, 4, 8, and 16 min) at -15°C. The monolith prepared with the shortest irradiation time (1.5 min) broke during the washing procedure and was washed out of the capillary. Therefore, the columns polymerized for the other time periods were evaluated. These prepared columns at -15°C were used to separate five alkylbenzenes (toluene to *n*-pentylbenzene) and  $t_0$  marker (uracil) in the isocratic mode, resulting in the observation of the chromatograms shown in Fig. 1. When the analytes were separated using the column polymerized for 16 min (Fig. 1b), terribly broadened peaks were obtained for alkylbenzenes. In contrast, the separation using the column polymerized for 2 min produced sharp peaks for all five alkylbenzenes (Fig. 1a). The relationship between polymerization time and theoretical plate numbers for uracil, toluene, and *n*-propylbenzene at a chromatographic linear flow velocity of 1.0 mm s<sup>-1</sup> are shown in Fig. 2. The column efficiencies for the retained analytes, toluene and *n*-propylbenzene, increased with decreasing polymerization time. The theoretical plate numbers for toluene and *n*-propylbenzene using the column polymerized for 2 min were 111000 and 105000 plates m<sup>-1</sup>, respectively. However, the column polymerized with 16 min UV irradiation exhibited deteriorated efficiencies, falling to 6300 and 4700 plates m<sup>-1</sup> for toluene and *n*-propylbenzene, respectively. For uracil, which was not retained on the column, the best efficiency was also achieved using the column polymerized for 2 min, and the lowest theoretical plate number was obtained with the column polymerized for 8 min. For columns prepared by UV photopolymerization at low temperatures, decreasing the polymerization time (and, consequently, monomer conversions) enhanced the separation efficiency in a manner analogous to that observed for thermal polymerization.<sup>24-26</sup>

Additionally, the monolithic columns polymerized at 0 and 15°C for 2 min were also prepared and evaluated under the

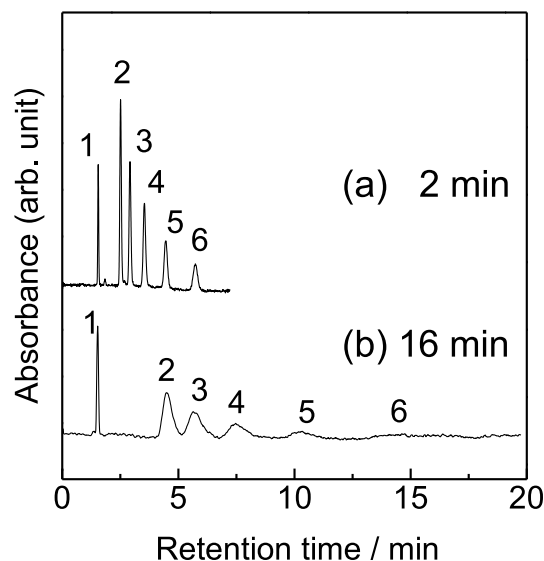


Fig. 1 Separation of alkylbenzenes at a linear flow rate of 1.0 mm s<sup>-1</sup> using the columns polymerized for 2 and 16 min at -15°C. Conditions: column length, 90 mm; mobile phase, 50:50 acetonitrile:water (v/v); analytes, (1) uracil ( $t_0$  marker), (2) toluene, (3) ethylbenzene, (4) *n*-propylbenzene, (5) *n*-butylbenzene, and (6) *n*-pentylbenzene; UV detection at 190 nm.

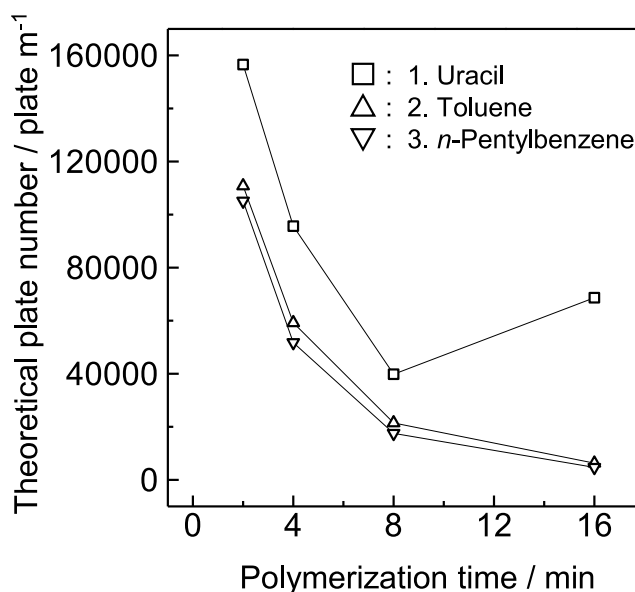


Fig. 2 Relationships between polymerization time and theoretical plate number for uracil, toluene, and *n*-propylbenzene using the columns polymerized for 2 - 16 min at -15°C; linear flow rate was 1.0 mm s<sup>-1</sup>.

same chromatographic conditions. The theoretical plate numbers for the alkylbenzenes were around 30000 plates m<sup>-1</sup> for 0°C and 5000 plates m<sup>-1</sup> for 15°C at a linear flow rate of 1 mm s<sup>-1</sup>. Moreover, an increase of polymerization temperature increased the flow resistance of the column; *i.e.*, the back pressure of the columns prepared at -15, 0, and 15°C were 0.14, 0.20, and 3.0 MPa, respectively, at a linear flow rate of 1 mm s<sup>-1</sup>. Since the objective of this study was preparation of highly efficient and low-flow resistant polymer monolithic column,

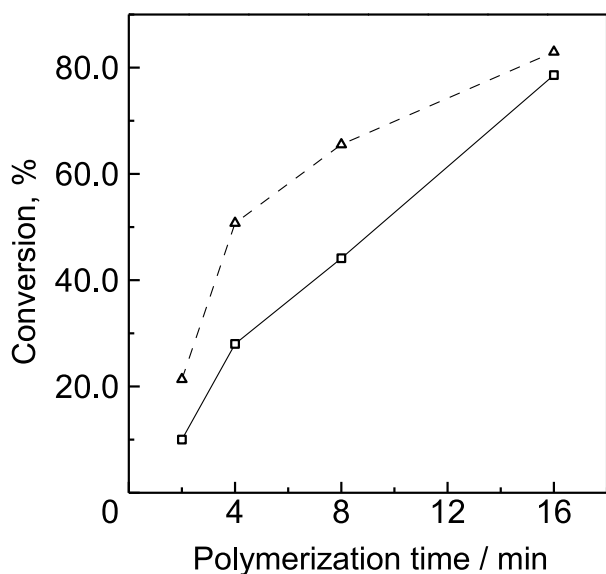


Fig. 3 Relationships between polymerization time and conversion of BMA ( $\square$ ) and EDMA ( $\triangle$ ) in the columns polymerized for 2 - 16 min at  $-15^{\circ}\text{C}$ .

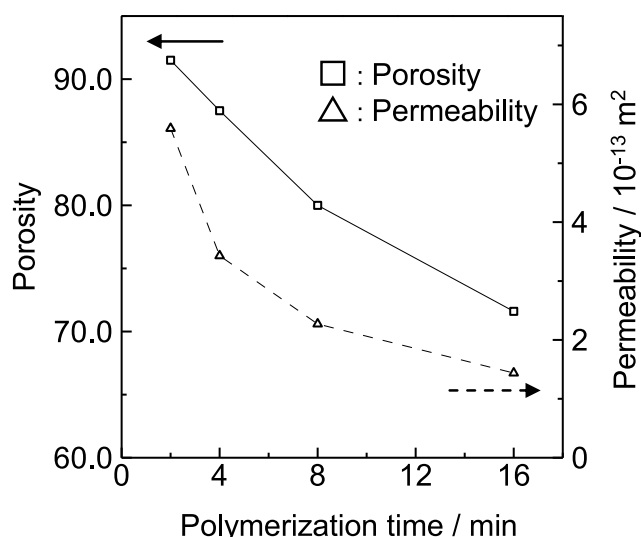


Fig. 4 Relationships between polymerization time and porosity ( $\square$ ) or permeability ( $\triangle$ ) of the columns polymerized for 2 - 16 min at  $-15^{\circ}\text{C}$ .

further investigations were focused on the columns prepared at  $-15^{\circ}\text{C}$ .

The conversion of both BMA and EDMA in the columns polymerized for 2, 4, 8, and 16 min at  $-15^{\circ}\text{C}$  was determined using Py-GC. Figure 3 shows the relationships between the polymerization time and the conversions of BMA and EDMA. Conversions for both constituents increased with increasing polymerization time. By UV irradiation for 2 min, the conversions of BMA and EDMA come around to 10 and 21%; for 16 min, they reached 79 and 83%, respectively. As clearly shown in Fig. 3, the polymerization of EDMA proceeded faster than that of BMA, which is consistent with previous reports.<sup>24-26</sup> At the shortest polymerization time, only about 6% of total monomer mass in the capillary ( $24 \text{ wt}\% \times 10\% + 16 \text{ wt}\% \times 21\%$ ) reacted to form the polymer monolith fixed in the capillary.

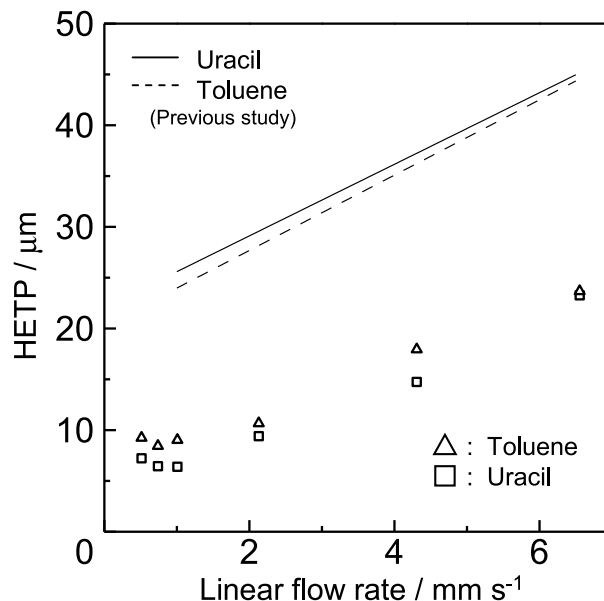


Fig. 5 Relationships between linear flow rate and the height equivalent to a theoretical plate (HETP) ( $H-u$  plots) for uracil and toluene. Chromatographic conditions were the same as those in Fig. 1.

The relationships between polymerization time and porosity/permeability of the monolith columns are shown in Fig. 4. The porosity  $\epsilon$ , which was directly affected by the extent of polymerization, decreased with increasing polymerization time. At the shortest polymerization time of 2 min, the porosity was determined to be 92%. Since the total monomer conversion at this condition was 6%, the porosity of 92%, or  $1 - \epsilon = 8\%$ , was considered a reasonable value.

The permeability of the columns polymerized at  $-15^{\circ}\text{C}$  determined using the elution time of  $t_0$  marker and Eq. (2) is also shown in Fig. 4. The permeability was increased with a decrease of the polymerization time, similarly to porosity. Polymerization for 2 min produced a column with a high permeability of  $5.6 \times 10^{-13} \text{ m}^2$ . This value is over an order of magnitude larger than that of a  $3\text{-}\mu\text{m}$  particle packed column and twice as large as that of the monolithic column prepared by UV irradiation in our previous study ( $2.0 \text{ mW cm}^{-2}$ , 8 min at  $0^{\circ}\text{C}$ ; %C: 32% for BMA, 58% for EDMA).<sup>21,31</sup>

The monolithic column polymerized for 2 min at  $-15^{\circ}\text{C}$  showed superior performance in terms of both separation efficiency and permeability. The characteristics of this column were further investigated. Figure 5 shows  $H-u$  plots for this column using symbols; along with the results for the column prepared in our previous study ( $2.0 \text{ mW}$ , 8 min,  $0^{\circ}\text{C}$ ) shown with lines for comparison. At a linear flow rate of  $1.0 \text{ mm s}^{-1}$ , the height equivalence to a theoretical plate (HETP) values for uracil and toluene were  $6.4$  and  $9.0 \mu\text{m}$ , respectively, using the column prepared in this study, while the values for the column in our previous study were approximately 2 - 3 times larger (about  $25 \mu\text{m}$  for uracil and  $22 \mu\text{m}$  for toluene). For the column in this study, the minimum HETPs were determined to be  $6.4 \mu\text{m}$  for uracil at a linear flow rate of  $1.0 \text{ mm s}^{-1}$  and  $8.4 \mu\text{m}$  for toluene at  $0.7 \text{ mm s}^{-1}$  toluene, corresponding to 157000 and 118000 plates  $\text{m}^{-1}$ , respectively. The  $H-u$  plots for the column in this study (marked by symbols in Fig. 5) are parallel to those for the column prepared previously (marked by lines) but are shifted down to lower HETP values in the range from 1.0 to  $6.5 \text{ mm s}^{-1}$ . This suggests that the reduction in the  $A$ -term in the

$H$ - $u$  plot can be achieved using the current column preparation method to cause greater homogeneity of the column structure.

The peak capacity,  $n$ , in an isocratic mode (ACN/water = 50/50, v/v) was also calculated by the following equation:<sup>32</sup>

$$n = 1 + \frac{\sqrt{N}}{4} \ln \left( \frac{t_R}{t_0} \right) \quad (4)$$

where  $N$ , and  $t_0$  and  $t_R$  are theoretical plate number, and retention time of the first and the last eluted peak, respectively. Here, the retention times of uracil and  $n$ -pentylbenzene were used as  $t_0$  and  $t_R$ , respectively, and the average theoretical plate number of uracil and  $n$ -pentylbenzene in each chromatogram was adopted as the  $N$  value. The  $n$  values obtained for the column in present and previous<sup>21</sup> works were almost comparable (34 and 33, respectively) because of the larger retention factor, or elution time, of  $n$ -pentylbenzene for the previous column ( $k = 6.4$ ) compared with that for the present one ( $k = 2.8$ ) in the same mobile phase condition.

CLSM observation was then performed to evaluate the morphology of the monolithic columns under the HPLC separation condition; *i.e.*, the columns used for the observation were filled with 50% ACN aqueous solution corresponding to the mobile phase used in this study. Figure 6 shows CLSM images of the longitudinal cross-section of the columns polymerized for (a) 2 min and (b) 16 min as well as (c) that of a column prepared under the conditions used in our previous study. The monolithic structure of the column polymerized for 2 min (Fig. 6a) was more homogeneous than that prepared in our previous study (Fig. 6c). Greater homogeneity should give rise to enhanced separation efficiency (Fig. 5) and a reduction in the  $A$ -term.

On the other hand, as shown in Fig. 6b, the density of the polymer monolith polymerized for 16 min appeared to be higher than that polymerized for 2 min (Fig. 6a), corresponding to the difference in monomer conversion. Meanwhile it seemed that the degree of homogeneity of the monolithic structures polymerized for 16 and 2 min observed in the CLSM images (Figs. 6(a) and 6(b)) were almost identical. As mentioned above, however, the theoretical plate numbers for the separation of toluene and  $n$ -propylbenzene using the column polymerized for 2 min were about 20 times larger than the corresponding values obtained for the column polymerized for 16 min. Here it should be noted that the copolymer composition of the monolith varied as the polymerization process proceeded as shown in Fig. 3. This fact suggests that compositional heterogeneity would increase with increasing monomer conversion, potentially leading to the decrease in the column efficiency for retained analytes. It was also reported that the specific surface area of the polymer monolith decreased with an increase of polymerization time.<sup>24-26,33</sup> Similar phenomenon would arise in the polymerization process in this work and affect separation efficiency. A detailed study to clarify the relation between the copolymer compositions of the monolith and column performance should be essential in the future work.

#### Repeatability, reproducibility, and stability of the low-flow-resistance column

The run-to-run repeatability, column-to-column reproducibility, and mechanical stability for the column polymerized for 2 min at  $-15^\circ\text{C}$  were evaluated. At the linear flow rate of  $1.0 \text{ mm s}^{-1}$ , the RSD for the run-to-run repeatability of retention time, retention factor, and HETP values for  $n$ -propylbenzene were 1, 1 and 5% ( $n = 3$ ), respectively. Moreover, the RSD for column-to-column reproducibility of the retention time,

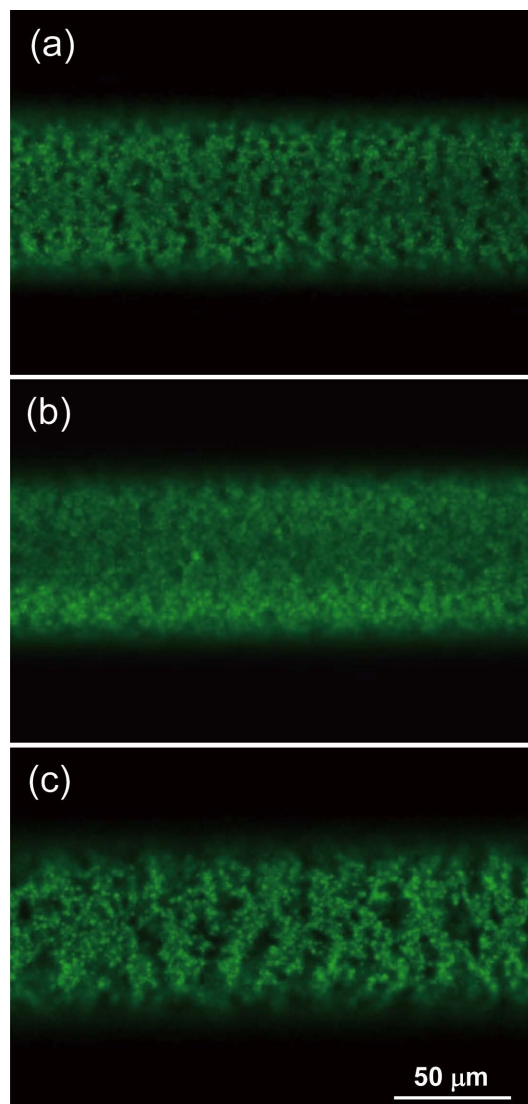


Fig. 6 CLSM images of longitudinal cross-sections of the columns polymerized for (a) 2 min and (b) 16 min at  $-15^\circ\text{C}$ , compared with (c) the column in our previous study.<sup>21</sup>

retention factor, and HETP values for  $n$ -propylbenzene at  $1.0 \text{ mm s}^{-1}$  were 4, 5 and 11%, respectively, and those of the flow resistance was within 9% ( $n = 4$ ).

In addition, the column was mechanically stable up to the linear flow rate at least  $16 \text{ mm s}^{-1}$  (1.9 MPa as back pressure); *i.e.*, a good linear relationship between the flow rate and back pressure was obtained (correlation coefficient = 0.999). Furthermore, no change in chromatographic property was observed during the continuous use of the column within at least a month.

#### Separations in vacuum pressure-driven HPLC

The low-flow-resistance polymer monolithic column with high separation efficiency was successfully prepared using 2 min polymerization at  $-15^\circ\text{C}$  as described in the previous section. The separation of alkylbenzenes using this low-flow-resistance column was then performed using a vacuum-driven HPLC in which a conventional HPLC pump was not used to generate the stream of the mobile phase. A direct injection method using suction ( $-0.045 \text{ MPa}$ , 10 s), similar to capillary electrophoresis (CE), was employed. After sample

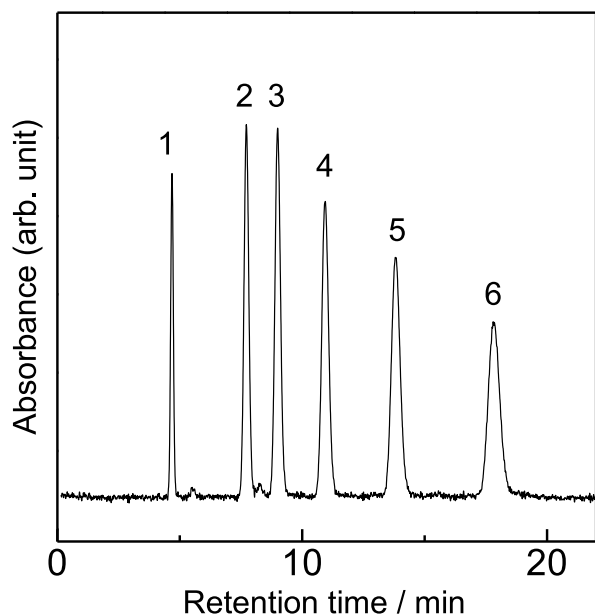


Fig. 7 Separation of alkylbenzenes using vacuum-driven HPLC. Pressure of vacuum:  $-0.045$  MPa. Other conditions were the same as those in Fig. 1.

loading, the mobile phase in the inlet reservoir was aspirated into the column by vacuum ( $-0.045$  MPa). As a result, the analytes were separated and detected as shown in Fig. 7. The sample solution was successfully injected and transferred to the outlet by the vacuum at the column outlet end. The flow rate under the vacuum was  $0.3 \text{ mm s}^{-1}$  and the separation efficiency was  $70000 - 85000 \text{ plates m}^{-1}$ . The RSDs for run-to-run repeatability of linear flow rate, the retention factor, and the HETP values for *n*-propylbenzene were 2, 0.3, and 1%, respectively ( $n = 3$ ). However, the RSD for the absolute peak height for *n*-propylbenzene was 24% ( $n = 3$ ). In contrast, the RSD for the relative peak height for *n*-propylbenzene to that for toluene was 2.2%. The insufficient precision in the injection volume resulting from the direct injection method was effectively corrected by the use of an internal standard. The vacuum-driven HPLC demonstrated high performance with good repeatability by using the low-flow-resistance column polymerized for 2 min at  $-15^\circ\text{C}$ .

## Conclusions

In this study, a low-flow-resistance poly(BMA-*co*-EDMA) monolithic column was successfully developed by combining low-conversion and low-temperature polymerization. A UV photopolymerization lasting 2 min was used to prepare the column at a low temperature of  $-15^\circ\text{C}$ . The column exhibited a high column efficiency of  $>100000 \text{ plates m}^{-1}$  with a high permeability of  $5.6 \times 10^{-13} \text{ m}^2$  in the RP-HPLC mode. CLSM images revealed that the prepared monolith structures were more homogenous than those prepared in our previous study. Compositional copolymerization homogeneity was apparently enhanced by reducing the polymerization time, and also improved the separation efficiency for retained analytes. Using the prepared column, a vacuum pressure-driven low-pressure HPLC system was used without the need for a conventional HPLC pump to separate five alkylbenzenes under a pressure of

$-0.045$  MPa. Additional research characterizing both the chemical and material properties of the monolith to understand their relationship to the separation efficiency is currently in progress in our laboratory, along with further applications of the low-pressure-HPLC.

## Supporting Information

Schematic illustration of a vacuum-driven HPLC system (Fig. S1). This material is available free of charge on the Web at <http://www.jsac.or.jp/analsci/>.

## References

1. C. Legido-Quigley, N. D. Marlin, V. Melin, A. Manz, and N. W. Smith, *Electrophoresis*, **2003**, *24*, 917.
2. G. Guiochon, *J. Chromatogr. A*, **2007**, *1168*, 101.
3. R. Wu, L. Hu, F. Wang, M. Ye, and H. Zou, *J. Chromatogr. A*, **2008**, *1184*, 369.
4. N. W. Smith and Z. Jiang, *J. Chromatogr. A*, **2008**, *1184*, 416.
5. D. Guillarme, J. Ruta, S. Rudaz, and J.-L. Veuthey, *Anal. Bioanal. Chem.*, **2010**, *397*, 1069.
6. H. Minakuchi, K. Nakanishi, N. Soga, N. Ishizuka, and N. Tanaka, *Anal. Chem.*, **1996**, *68*, 3498.
7. K. Cabrera, *J. Sep. Sci.*, **2004**, *27*, 843.
8. O. Núñez, K. Nakanishi, and N. Tanaka, *J. Chromatogr. A*, **2008**, *1191*, 231.
9. F. Svec and J. M. J. Fréchet, *Anal. Chem.*, **1992**, *64*, 820.
10. K. Hosoya, N. Hira, K. Yamamoto, M. Nishimura, and N. Tanaka, *Anal. Chem.*, **2006**, *78*, 5729.
11. Z. Kučerová, M. Szumski, B. Buszewski, and P. Jandera, *J. Sep. Sci.*, **2007**, *30*, 3018.
12. H. Aoki, N. Tanaka, T. Kubo, and K. Hosoya, *J. Sep. Sci.*, **2009**, *32*, 341.
13. M. W. H. Roberts, C. M. Ongkudon, G. M. Forde, and M. K. Danquah, *J. Sep. Sci.*, **2009**, *32*, 2485.
14. E. G. Vlakh and T. B. Tennikova, *J. Chromatogr. A*, **2009**, *1216*, 2637.
15. F. Svec, *J. Chromatogr. A*, **2010**, *1217*, 902.
16. F. Svec, *J. Chromatogr. A*, **2012**, *1228*, 250.
17. K. Miyamoto, T. Hara, H. Kobayashi, H. Morisaka, D. Tokuda, K. Horie, K. Koduki, S. Makino, O. Núñez, C. Yang, T. Kawabe, T. Ikegami, H. Takubo, Y. Ishihama, and N. Tanaka, *Anal. Chem.*, **2008**, *80*, 8741.
18. M. Iwasaki, S. Miwa, T. Ikegami, M. Tomita, N. Tanaka, and Y. Ishihama, *Anal. Chem.*, **2010**, *82*, 2616.
19. D. Lee, F. Svec, and J. M. J. Fréchet, *J. Chromatogr. A*, **2004**, *1051*, 53.
20. Y. Ueki, T. Umemura, Y. Iwashita, T. Otake, H. Haraguchi, and K. Tsunoda, *J. Chromatogr. A*, **2006**, *1106*, 106.
21. T. Hirano, S. Kitagawa, and H. Ohtani, *Anal. Sci.*, **2009**, *25*, 1107.
22. M. Takahashi, T. Hirano, S. Kitagawa, and H. Ohtani, *J. Chromatogr. A*, **2012**, *1232*, 123.
23. I. K. Kiplagat, P. Kubáň, P. Pelcová, and V. Kubáň, *J. Chromatogr. A*, **2010**, *1217*, 5116.
24. L. Trojer, C. P. Bisjak, W. Wieder, and G. K. Bonn, *J. Chromatogr. A*, **2009**, *1216*, 6303.
25. I. Nischang and O. Brüggemann, *J. Chromatogr. A*, **2010**, *1217*, 5389.
26. I. Nischang, I. Teasdale, and O. Brüggemann, *J. Chromatogr. A*, **2010**, *1217*, 7522.

27. M. Szumski and B. Buszewski, *J. Sep. Sci.*, **2009**, 32, 2574.
  28. P. Carman, "*Flow of Gases through Porous Media*", **1956**, Butterworth, London.
  29. H. Saito, K. Kanamori, K. Nakanishi, and K. Hirao, *J. Sep. Sci.*, **2007**, 30, 2881.
  30. S. Bruns, T. Müllner, M. Kollmann, J. Schachtner, A. Hölzel, and U. Tallarek, *Anal. Chem.*, **2010**, 82, 6569.
  31. T. Nakaza, A. Kobayashi, T. Hirano, S. Kitagawa, and H. Ohtani, *Anal. Sci.*, **2012**, 28, 917.
  32. J. C. Giddings, *Anal. Chem.*, **1967**, 39, 1027.
  33. F. Svec and J. M. J. Fréchet, *Chem. Mater.*, **1995**, 7, 707.
-